Journal of Elasticity, Vol. 9, No. 4, October 1979

Alphen aan den Rijn
Printed in the Netherlands

Loss of adhesion at the tip of an interface crack

J. D. ACHENBACH, L. M. KEER, R. P. KHETAN,* and S. H. CHEN

Department of Civil Engineering, The Technological Institute, Northwestern University, Evanston, Illinois 60201, U.S.A.

(Received November 29, 1978)

ABSTRACT

A model is constructed to analyze adhesive bond failure at the tip of an interface crack. The model is based on the assumption that there are zones of bounded cohesive tensile and shear stresses near a crack tip. Within the context of certain broad a-priori assumptions on the distributions of certain stress and displacement components in the cohesive zones, the requirement that *all* stresses in the two materials remain bounded provides a method to compute the specific details for these zones. It is assumed that bond failure occurs when the extension of the bond fiber at the crack tip exceeds a critical value. For an interface crack in a uniform tension field computations for two alternate formulations suggest that this failure criterion is independent of the precise distribution of the cohesive stresses, but rather depends only upon their averaged values. Combined loading with a dominant tensile component has also been analyzed. If the critical extension of bond fibers and the maximum value of the cohesive tensile stress are known, the model provides the maximum allowable interface stresses for given crack dimension and material parameters.

1. Introduction

The work presented here has two primary goals: first to establish a relatively simple model for the analysis of bond stresses and deformations near an interface crack between two materials and secondly, to establish a criterion for propagation of an interface crack. The understanding of the failure mechanism for interface cracks has important practical use in numerous engineering applications.

From the analytical point of view, the general character of the fields of stresses and displacements near the tip of an interface crack depends on the manner in which the conditions change from the interface bond to the crack faces. Usually it is assumed that a single point of singularity (the crack tip) forms the transition from continuous stresses and displacements ahead of the crack tip (perfect bond) to traction-free conditions on the crack faces. Unfortunately a single point of transition gives rise to oscillatory singularities in the stress field. Furthermore, there will be a wrinkling of the materials near the crack tip causing them to overlap in a small vicinity near the tip. This feature of the interface crack has been pointed out by

* Former post-doctoral fellow and now at General Motors Research Laboratories, Warren, Michigan, 48090.

England [1] and by Malyshev and Salganik [2]. For an interface crack in a tensile field, Comninou [3] has only recently removed these undesirable aspects of the solution by introducing three regions in solving the problem of an interface crack. One region is a fully bonded one in which stresses and displacements are continuous, a very small region at the crack tip is treated as in a contact problem, preserving continuity of normal displacements while specifying zero shear, and finally, there is the region of the loaded (or stress-free) crack faces. The solution obtained in this manner is satisfactory from many standpoints and it does not lead to a contradictory solution having overlapping crack faces. From a physical standpoint it has the drawback that the contact zone is about 10^{-4} to 10^{-7} times the length of the crack which is probably small enough to violate assumptions concerning the use of a continuum model. If one considers an interface crack in shear, the problem becomes still considerably more complicated. This is due to the fact that the jumps in the normal displacements are antisymmetric about the origin so that a relatively large portion of the crack will overlap. Comninou [4] has also considered this problem and established a solution similar to the previous one. However, in this case one of the contact zones is about half the size of the crack, while the other is less than 10^{-7} times the crack length. It should be noted that Comninou has again assumed that all contact zones are free of shear stresses. Generally this is not true in the actual case, but the introduction of some type of friction mechanism would introduce mathematical complications as well as questions of a physical nature since the friction mechanism would be conjectural.

A model that may be more realistic for interface cracks is one in which the bond in a small zone near the crack tip is allowed to yield under the high stresses that are to be expected near an interface flaw. Since this yielding may be assumed to take place in an infinitesimally thin zone (the interface) it can very conveniently be related to an appropriate distribution of cohesive tractions, which is then defined by the nature of the adhesive bond. For a homogeneous solid such a cohesive tractions model has been discussed by Barenblatt [5], with the basic idea that through the use of a zone of cohesive forces, the singularity at the crack tip can be eliminated. A similar idea was previously used by Dugdale [6], who considered all stresses in the line of the crack to be bounded by a maximum yield stress *in tension* and through this mechanism was able to determine the size of the yield zones. This same idea was also applied by Bilby, Cottrell, and Swinden [7] to cracks using concepts from dislocation theory. These authors postulated a failure criterion that depended upon the value of the crack opening displacement at the tip of the crack. It should be noted that the above criteria have been applied to cracks in a single material where the loading mechanism is either mode I (Barenblatt, Dugdale) or mode III (Bilby, Cottrell, and Swinden).

The formulation for the model discussed here is as follows: *either* normal or tangential cohesive stresses are introduced (see Figure 1) in regions $a<x<L_2$ and $-L_1<x<-a$; regions $x>L_2$ and $x<-L_1$ have continuous displacements and stresses; and stresses corresponding to the external loads are prescribed in $|x|<a$. Since the cohesive zones are small transition zones it is convenient to prescribe

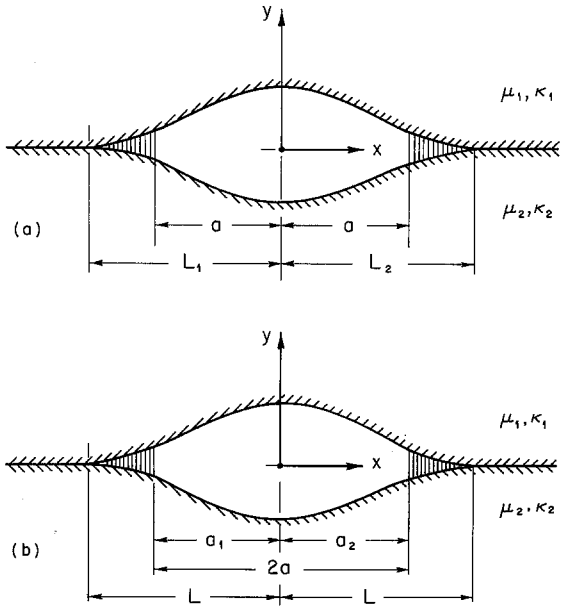

Figure 1. Geometry and coordinate system for the interface crack.

either (a): a distribution of cohesive normal stresses (CNS) and a tangential interface separation of prescribed general form (CNS formulation), or (b): a distribution of cohesive shear stresses (CSS) and a normal interface separation of prescribed form (CSS formulation). By prescribing the conditions in the cohesive zones according to (a) or (b), oscillatory singularities do not occur. In addition it is required that there will not be singularities of other kinds. The latter condition is met if the stresses are continuous over the entire region of the interface crack. Thus, we require that the normal stress and tangential interface separation (CNS formulation) and the shear stress and normal interface separation (CSS formulation) possess sufficient continuity by suitable restriction of the quantities in the cohesive zones. In this paper such continuity is achieved by taking triangular distributions of cohesive stresses and smooth interface separations with one adjustable parameter.

As fracture criterion we adopt that the elongation of the bond fiber at the trailing edge of the cohesive zone (which corresponds to the crack opening displacement at that point) must exceed a critical value for propagation of the crack. For the case of tension it is shown that (when properly normalized) the crack opening displacement has the same value for the CNS formulation (a) and the CSS formulation (b).

In Section 2 the problem of the interface crack with cohesive zones in a tensile field is formulated, for the case that normal cohesive stresses and tangential interface separations are specified in the cohesive zone. The governing integral equations are solved and the lengths of the cohesive zones as well as the constant in the distribution of the interface separation are computed. The CSS formulation and solution are presented in Section 4. Numerical results for both the CNS and CSS

formulations are given in Section 5. The case of pure shear loading is briefly discussed in Section 6, but is not pursued in detail. Combined loading with a dominant tensile component is analysed in Section 7 for the CNS formulation. Numerical results for that case are presented in Section 8, and the results are discussed in some detail.

2. Pressure loading–CNS formulation

In this section a line crack in the interface between two bonded half-planes is considered. The faces of the crack are subjected to uniform pressures σ_0. It follows from superposition considerations that the solution applies to an interface crack in a uniform tensile field which is directed normal to the interface. We assume that yielding in the interface is resisted by cohesive tractions similar to the ones introduced by Dugdale and by Bilby, Cottrell, and Swinden. The geometry and coordinate system for such an interface crack are shown in Figure 1a, where the crack length is given by 2a and the cohesive zones by L_2-a and L_1-a. The material constants are μ_j and κ_j, where $j=1, 2$, refers to the upper and lower half-planes, respectively, and $\kappa=3-4\nu$ (plane strain) or $(3-\nu)/(1+\nu)$ (plane stress), where ν is Poisson's ratio. Because of symmetry we have $L_1=L_2=L$. This symmetry will not hold in Sections 7 and 8.

The boundary conditions for the present problem are

$$|x|<a,\ y=0: \qquad \sigma_y^1=\sigma_y^2=-\sigma_0; \qquad \sigma_{xy}^1=\sigma_{xy}^2=0 \tag{2.1a,b}$$

$$a<|x|<L,\ y=0: \qquad \sigma_y^1=\sigma_y^2=T\frac{|x|-a}{L-a}-\sigma_0 \tag{2.2}$$

$$\frac{\partial}{\partial x}(u_x^1-u_x^2)=-A(1-x^2/L^2)^{1/2} \tag{2.3}$$

$$|x|>L,\ y=0: \qquad u_y^1=u_y^2; \qquad u_x^1=u_x^2 \tag{2.4a, b}$$

$$|x|>0,\ y=0: \qquad \sigma_y^1=\sigma_y^2; \qquad \sigma_{xy}^1=\sigma_{xy}^2 \tag{2.5a,b}$$

where superscripts "1" and "2" refer to the upper and lower half-plane, respectively. The stresses and displacements are denoted by σ_x, σ_y, σ_{xy}, and u_x, u_y, respectively. The uniform tension is introduced into the boundary conditions as a compressive stress σ_0 applied to the faces of the crack; σ_0 is assumed to act on the crack face, $|x|<a$, and in the cohesive zones, $a<|x|<L$. The cohesive tractions, which are tensile, are assumed to be *linear* and have a maximum amplitude T at $x=\pm L$, (see equation (2.2)). The tangential interface separation is given in the form shown in equation (2.3), which eliminates all singularities at $x=\pm L$. The constant A is as yet undetermined and will be found from the condition that there are no singularities at $x=\pm a$. The present problem is called CNS because the form of the normal cohesive tractions is prescribed for the case of applied normal loading, in addition the form of the tangential displacement jumps is prescribed. In a subsequent section the CSS

problem will be solved. In that case for the applied normal loading the forms of cohesive shear tractions and the normal displacement jumps will be prescribed.

It is convenient to represent displacements and stresses in the form of Fourier transforms as follows:

$$2\mu_j u_x^j = \frac{\mp i}{(8\pi)^{1/2}} \int_{-\infty}^{\infty} \{[(\kappa_j - 1) \mp 2|\xi| y] C_j(\xi) + [(\kappa_j + 1) \operatorname{sgn}(\xi) \mp 2\xi y] D_j(\xi)\} e^{-i\xi x} e^{\mp|\xi| y} \, d\xi \tag{2.6}$$

$$2\mu_j u_y^j = \frac{1}{(8\pi)^{1/2}} \int_{-\infty}^{\infty} \{[(\kappa_j + 1) \operatorname{sgn}(\xi) \pm 2\xi y] C_j(\xi) + [(\kappa_j - 1) \pm 2|\xi| y] D_j(\xi)\} \times e^{-i\xi x} e^{\mp|\xi| y} \, d\xi \tag{2.7}$$

$$\sigma_y^j = \frac{\mp 1}{(2\pi)^{1/2}} \int_{-\infty}^{\infty} \xi \{(1 \pm |\xi| y) C_j(\xi) \pm \xi y D_j(\xi)\} e^{-i\xi x} e^{\mp|\xi| y} \, d\xi \tag{2.8}$$

$$\sigma_{xy}^j = \frac{i}{(2\pi)^{1/2}} \int_{-\infty}^{\infty} \xi \{\mp \xi y C_j(\xi) + (1 \mp |\xi| y) D_j(\xi)\} e^{-i\xi x} e^{\mp|\xi| y} \, d\xi \tag{2.9}$$

$$\sigma_x^j = \frac{1}{(2\pi)^{1/2}} \int_{-\infty}^{\infty} \xi (\{(\mp 1 + |\xi| y) C_j(\xi) + [\mp 2 \operatorname{sgn}(\xi) + \xi y] D_j(\xi)\} e^{-i\xi x} e^{\mp|\xi| y} \, d\xi \tag{2.10}$$

Here the upper sign applies for the upper half-plane ($j = 1$), and the lower sign for the lower half-plane ($j = 2$). The functions $C_j(\xi)$ and $D_j(\xi)$ are as yet unknown functions of ξ. Because of the symmetry of the problem, Eqs. (2.6)–(2.10) can be written as Fourier sine or cosine transforms (e.g. u_x, u_y become sine and cosine transforms respectively). Through the use of boundary conditions (2.5a,b), functions $C_2(\xi)$ and $D_2(\xi)$ can be eliminated in favor of $C_1(\xi)$ and $D_1(\xi)$; the remaining boundary conditions lead to the following integral equations:

$$\left(\frac{2}{\pi}\right)^{1/2} \int_0^{\infty} \xi C_1(\xi) \cos(\xi x) \, d\xi = \begin{cases} \sigma_0, & |x| < a \\ \sigma_0 - T\dfrac{|x| - a}{L - a}, & a < |x| < L \end{cases} \tag{2.11}$$

$$\left(\frac{2}{\pi}\right)^{1/2} \int_0^{\infty} \xi D_1(\xi) \sin(\xi x) \, d\xi = 0, \qquad |x| < a \tag{2.12}$$

$$\left(\frac{2}{\pi}\right)^{1/2} \frac{1}{4\mu_1} \int_0^{\infty} \{[(\kappa_1 + 1) + \Gamma(\kappa_2 + 1)] C_1(\xi) + [(\kappa_1 - 1) - \Gamma(\kappa_2 - 1)] D_1(\xi)\} \cos(\xi x) \, d\xi = 0, \qquad |x| > L \tag{2.13}$$

$$-\left(\frac{2}{\pi}\right)^{1/2} \frac{1}{4\mu_1} \int_0^{\infty} \{[(\kappa_1 - 1) - \Gamma(\kappa_2 - 1)] C_1(\xi) + [(\kappa_1 + 1) + \Gamma(\kappa_2 + 1)] D_1(\xi)\} \sin(\xi x) \, d\xi = \begin{cases} 0, & |x| > L \\ -A(1 - x^2/L^2)^{1/2}, & a < |x| < L \end{cases} \tag{2.14}$$

If we define

$$C_1(\xi) = \alpha M(\xi) + \beta N(\xi) \operatorname{sgn}(\xi) \tag{2.15}$$

$$D_1(\xi) = -\beta M(\xi) \operatorname{sgn}(\xi) - \alpha N(\xi) \tag{2.16}$$

where

$$\frac{\alpha}{\mu_1} = \frac{\kappa_1 - 1 - \Gamma(\kappa_2 - 1)}{(\kappa_1 + \Gamma)(1 + \kappa_2 \Gamma)} \tag{2.17}$$

$$\frac{\beta}{\mu_1} = \frac{\kappa_1 + 1 + \Gamma(\kappa_2 + 1)}{(\kappa_1 + \Gamma)(1 + \kappa_2 \Gamma)} \tag{2.18}$$

and

$$\Gamma = \mu_1/\mu_2 \tag{2.19}$$

Then the boundary conditions will yield a set of coupled pairs of dual integral equations for the unknown functions, M and N, as given below:

$$\left(\frac{2}{\pi}\right)^{1/2} \int_0^\infty M(\xi) \sin(\xi x)\, d\xi = 0, \qquad |x| > L \tag{2.20}$$

$$\left(\frac{2}{\pi}\right)^{1/2} \int_0^\infty N(\xi) \cos(\xi x)\, d\xi = 0, \qquad |x| > L \tag{2.21}$$

$$\left(\frac{2}{\pi}\right)^{1/2} \frac{\partial}{\partial x} \int_0^\infty M(\xi) \sin(\xi x)\, d\xi = -A(1 - x^2/L^2)^{1/2}, \qquad a < |x| < L \tag{2.22}$$

$$-\left(\frac{2}{\pi}\right)^{1/2} \int_0^\infty [\beta M(\xi) + \alpha N(\xi)] \xi \sin(\xi x)\, d\xi = 0, \qquad |x| < a \tag{2.23}$$

$$\left(\frac{2}{\pi}\right)^{1/2} \int_0^\infty [\alpha M(\xi) + \beta N(\xi)] \xi \cos(\xi x)\, d\xi = \begin{cases} \sigma_0, & |x| < a \\ \sigma_0 - T\dfrac{|x| - a}{L - a}, & a < |x| < L \end{cases} \tag{2.24}$$

We note that equations (2.20)–(2.24) provide two equations each for the regions, $|x| < a$ (crack), $a < |x| < L$ (cohesive zone), $|x| > L$ (perfect bond). The next step in the procedure is to solve equations (2.20)–(2.24) by representing them in the form of singular integral equations. Therefore, define the dislocation densities, $b_1(x)$ and $b_2(x)$, in terms of the following integral transforms:

$$\left(\frac{2}{\pi}\right)^{1/2} \int_0^\infty \xi N(\xi) \sin(\xi x)\, d\xi = -b_1(x) H(L - |x|) \tag{2.25}$$

$$\left(\frac{2}{\pi}\right)^{1/2} \int_0^\infty \xi M(\xi) \cos(\xi x)\, d\xi = b_2(x) H(L - |x|) \tag{2.26}$$

where H is the Heaviside function and

$$\xi M(\xi) = \left(\frac{2}{\pi}\right)^{1/2} \int_0^L b_2(t) \cos(\xi t)\, dt \tag{2.27}$$

$$\xi N(\xi) = -\left(\frac{2}{\pi}\right)^{1/2} \int_0^L b_1(t) \sin(\xi t)\, dt \tag{2.28}$$

Substituting for M and N (equations (2.27), (2.28)) and noting that equations (2.20), (2.21) are automatically satisfied, one finds the following singular integral equations for the remaining equations, (2.22)–(2.24):

$$\alpha b_2(x)-\frac{\beta}{\pi}\int_{-L}^{L}\frac{b_1(t)\,dt}{t-x}=\begin{cases}\sigma_0, & |x|<a\\ \sigma_0-T\dfrac{|x|-a}{L-a}, & a<|x|<L\end{cases} \tag{2.29}$$

$$\alpha b_1(x)+\frac{\beta}{\pi}\int_{-L}^{L}\frac{b_2(t)\,dt}{t-x}=0, \qquad |x|<a \tag{2.30}$$

$$b_2(x)=-A(1-x^2/L^2)^{1/2}, \qquad a<|x|<L \tag{2.31}$$

Physical quantities can be readily obtained. From the definition of dislocation densities

$$\frac{\partial}{\partial x}(u_x^1-u_x^2)=b_2(x)[H(x+L)-H(x-L)] \tag{2.32}$$

$$\frac{\partial}{\partial x}(u_y^1-u_y^2)=b_1(x)[H(x+L)-H(x-L)] \tag{2.33}$$

the actual displacement jumps across the crack can be calculated by a simple quadrature. The stresses along the entire interface $-\infty<x<\infty$, $y=0$ are given as

$$\sigma_y^1=\sigma_y^2=-\alpha b_2(x)+\frac{\beta}{\pi}\int_{-L}^{L}\frac{b_1(t)\,dt}{t-x} \tag{2.34}$$

$$\sigma_{xy}^1=\sigma_{xy}^2=\alpha b_1(x)+\frac{\beta}{\pi}\int_{-L}^{L}\frac{b_2(t)\,dt}{t-x} \tag{2.35}$$

They will be put into a more explicit form in the next section.

Equations (2.29)–(2.31) can be put into dimensionless form by making the following substitutions

$$\tilde{x}=x/L,\ \tilde{a}=a/L,\ \tilde{T}=T/\sigma_0$$
$$\tilde{b}_2=\beta b_2/\sigma_0,\ \tilde{b}_1=\beta b_1/\sigma_0,\ \tilde{A}=A\beta/\sigma_0,$$
$$\tilde{\beta}=\alpha/\beta \quad \text{(Dundurs' constant)} \tag{2.36}$$

For the sake of convenience the notation $(\sim)$ is dropped and subsequent equations will be in dimensionless form and can be returned to dimensional form through the use of equations (2.36). Equations (2.29)–(2.31) become

$$\beta b_2(x)-\frac{1}{\pi}\int_{-1}^{1}\frac{b_1(t)\,dt}{t-x}=\begin{cases}1, & |x|<a\\ 1-T\dfrac{|x|-a}{1-a}, & a<|x|<1\end{cases} \tag{2.37}$$

$$\beta b_1(x)+\frac{1}{\pi}\int_{-1}^{1}\frac{b_2(t)\,dt}{t-x}=0, \qquad |x|<a \tag{2.38}$$

$$b_2(x)=-A(1-x^2)^{1/2}, \qquad a<|x|<1 \tag{2.39}$$

Solutions will be sought for which $b_1(\pm 1)$ and $b_2(\pm a)$ are bounded.

3. CNS formulation-solution of integral equations

To prepare equations (2.37)–(2.39) for numerical solution it is essential to write them as a single singular integral equation. Thus, write equation (2.37) as

$$\frac{1}{\pi}\int_{-1}^{1}\frac{b_1(t)\,dt}{t-x}=\beta b_2(x)-1+H(|x|-a)T\frac{|x|-a}{1-a} \tag{3.1}$$

where for $b_1(t)$ to be bounded at $t=\pm 1$, we require the following condition to be satisfied:

$$\frac{\beta}{\pi}\int_{-1}^{1}\frac{b_2(x)\,dx}{(1-x^2)^{1/2}}+\frac{2T}{\pi(1-a)}[(1-a^2)^{1/2}-a\cos^{-1}a]-1=0 \tag{3.2}$$

A bounded solution to equation (3.1) can be written (see, e.g. Muskhelishvili [8]) as

$$b_1(s)=-\frac{\beta(1-s^2)^{1/2}}{\pi}\int_{-1}^{1}\frac{b_2(x)\,dx}{(1-x^2)^{1/2}(x-s)}-\frac{T}{\pi(1-a)}$$
$$\times\left[(s-a)\ln\frac{1-as+[(1-a^2)(1-s^2)]^{1/2}}{|a-s|}+(s+a)\ln\frac{1+as+[(1-a^2)(1-s^2)]^{1/2}}{|a+s|}\right]$$
$$|s|<1 \tag{3.3}$$

Substituting for $b_1(s)$ in equation (2.38) and rearranging the terms, we obtain

$$\frac{1}{\pi}\int_{-1}^{1}\left\{1-\beta^2\left[\frac{1-s^2}{1-x^2}\right]^{1/2}\right\}\frac{b_2(x)\,dx}{x-s}=\frac{\beta T}{\pi(1-a)}$$
$$\left[(s-a)\ln\frac{1-as+[(1-a^2)(1-s^2)]^{1/2}}{a-s}+(s+a)\ln\frac{1+as+[(1-a^2)(1-s^2)]^{1/2}}{a+s}\right]$$
$$|s|<a \tag{3.4}$$

which along with equation (2.39) provides the desired singular integral equation. In addition, since the total slip must vanish, we have

$$\frac{1}{\pi}\int_{-1}^{1}b_2(s)\,ds=0 \tag{3.5}$$

Equations (3.2), (3.5) permit the determination of two of the three parameters T, a, and A. In practice, T, the maximum cohesive stress normalized with respect to the applied loading, is given; the other two parameters, a and A, can be obtained from the solution to the problem. However, since the problem is nonlinear in a, for convenience in the numerical calculations we prescribe a, and solve for $b_2(x)$, T and A.

To prepare the problem for numerical analysis we note that the function $b_2(s)$ can be expressed in the following form:

$$b_2(s)=\begin{cases}f(s)-A(1-a^2)^{1/2}, & |s|<a\\ -A(1-s^2)^{1/2}, & a<|s|<1\end{cases} \tag{3.6}$$

For continuity of $b_2(s)$, the function, $f(s)$, must vanish at $s=\pm a$, and it will be shown

later that this does indeed happen. Equation (2.39) is automatically satisfied, and equation (3.4) yields

$$\frac{1}{\pi}\int_{-1}^{1}\frac{f(x^*)\,dx^*}{x^*-s^*}\left\{1-\beta^2\left[\frac{1-s^2}{1-x^2}\right]^{1/2}\right\}=AF(s)+TG(s),\qquad |s|,|x|<a \tag{3.7}$$

where

$$F(s)=\frac{1}{\pi}\left\{[(1-s^2)^{1/2}-(1-a^2)^{1/2}](1-\beta^2)\ln\frac{a+s}{a-s}\right.$$
$$+[\beta^2(1-a^2)^{1/2}+(1-s^2)^{1/2}]\ln\frac{1-as+[(1-a^2)(1-s^2)]^{1/2}}{1+as+[(1-a^2)(1-s^2)]^{1/2}}$$
$$\left.-\beta^2(1-s^2)^{1/2}\ln\frac{1-s}{1+s}-2s\cos^{-1}a\right\} \tag{3.8}$$

$$G(s)=\frac{\beta}{\pi(1-a)}\left[(s-a)\ln\frac{1-as+[(1-a^2)(1-s^2)]^{1/2}}{a-s}\right.$$
$$\left.+(s+a)\ln\frac{1+as+[(1-a^2)(1-s^2)]^{1/2}}{a+s}\right] \tag{3.9}$$

and

$$s^*=s/a,\qquad x^*=x/a \tag{3.10}$$

We note that the right-hand side of equation (3.7) is bounded and continuous and equation (3.7) can be rewritten as

$$\frac{1-\beta^2}{\pi}\int_{-1}^{1}\frac{f(x^*)\,dx^*}{x^*-s^*}+\frac{\beta^2}{\pi}\int_{-1}^{1}\frac{1-[(1-s^2)/(1-x^2)]^{1/2}}{x^*-s^*}f(x^*)\,dx^*$$
$$=AF(s)+TG(s)\qquad |s^*|<1 \tag{3.11}$$

Equation (3.11) is a singular integral equation of the first kind since the kernel in the second integral is bounded. Bounded solutions for $f(x^*)$ do exist since the consistency condition is automatically satisfied. (We note that $F(s)$, $G(s)$ and the second integral on the left of (3.7) are all antisymmetric in s. Furthermore, $f(x^*)$ is an even function in x^*, due to the symmetry of the problem.)

Substituting equation (3.6) into conditions (3.2) and (3.5) allow them to be written as

$$\frac{\beta a}{\pi}\int_{-1}^{1}\frac{f(x^*)\,dx^*}{(1-x^2)^{1/2}}-\frac{2A\beta}{\pi}\{(1-a^2)^{1/2}\sin^{-1}a+(1-a)\}-1$$
$$+\frac{2T}{\pi(1-a)}[(1-a^2)^{1/2}-a\cos^{-1}a]=0 \tag{3.12}$$

and

$$\frac{a}{\pi}\int_{-1}^{1}f(x^*)\,dx^*-\frac{A}{\pi}[a(1-a^2)^{1/2}+\cos^{-1}a]=0 \tag{3.13}$$

Equations (3.11), (3.12) and (3.13) are now ready for numerical analysis and they can be discretized as follows:

$$\sum_{i=1}^{N} \frac{f(x_i^*)2s_k^*(1-x_i^{*2})^{1/2}}{(2N+1)(x_i^{*2}-s_k^{*2})}\left[1-\frac{\beta^2(1-a^2s_k^{*2})^{1/2}}{(1-a^2x_i^{*2})^{1/2}}\right]=AF(as_k^*) + TG(as_k^*) \qquad k=1,2,\ldots N \tag{3.14}$$

$$\frac{2\beta a}{2N+1}\sum_{i=1}^{N}\frac{f(x_i^*)(1-x_i^{*2})^{1/2}}{(1-a^2x_i^{*2})^{1/2}}-\frac{2A\beta}{\pi}[(1-a^2)^{1/2}\sin^{-1}a+(1-a)]-1 + \frac{2T}{\pi(1-a)}[(1-a^2)^{1/2}-a\cos^{-1}a]=0 \tag{3.15}$$

$$\frac{2a}{2N+1}\sum_{i=1}^{N} f(x_i^*)(1-x_i^{*2})^{1/2}-\frac{A}{\pi}[a(1-a^2)^{1/2}+\cos^{-1}a]=0 \tag{3.16}$$

where

$$x_i^*=\cos\frac{\pi i}{2N+1}, \qquad i=1,2,\ldots N \tag{3.17}$$

$$s_k^*=\cos\frac{\pi(k-0.5)}{2N+1}, \quad k=1,2,\ldots N \tag{3.18}$$

Equations (3.14)–(3.18) provide the basis by which the unknown quantities can be calculated, i.e. the function, $f(x)$, and parameters, T and A. We also note that the problem is nonlinear in the parameter a.

The physical quantities to be determined are the displacement slopes and the stresses in the cohesive zone. From the former the displacements may be calculated by a direct quadrature. The displacement slopes are given by the following equations.

$$b_1(s)=\frac{\beta(1-s^2)^{1/2}}{\pi}\int_{-1}^{1}\frac{f(x^*)}{(1-a^2x^{*2})^{1/2}}\frac{dx^*}{x^*-s^*}-\frac{\beta A}{\pi}\left\{\left[(1-a^2)^{1/2} -(1-s^2)^{1/2}\right]\ln\left|\frac{a+s}{a-s}\right|+(1-a^2)^{1/2}\ln\frac{1-as+[(1-a^2)(1-s^2)]^{1/2}}{1+as+[(1-a^2)(1-s^2)]^{1/2}} -(1-s^2)^{1/2}\ln\frac{1-s}{1+s}\right\} -\frac{T}{\pi(1-a)}\left[(s-a)\ln\frac{1-as+[(1-a^2)(1-s^2)]^{1/2}}{|a-s|} +(s+a)\ln\frac{1+as+[(1-a^2)(1-s^2)]^{1/2}}{|a+s|}\right] \tag{3.19}$$

$$b_2(x)=\begin{cases} f(x^*)-A(1-a^2)^{1/2}, & |x|<a \\ -A(1-x^2)^{1/2}, & a<|x|<1 \end{cases} \tag{3.20}$$

The stresses in the cohesive zone can be written as follows:

$$\frac{\sigma_y}{\sigma_0} = -1 + T\frac{|s|-a}{1-a} \qquad a<|s|<1 \tag{3.21}$$

$$\frac{\sigma_{xy}}{\sigma_0} = \frac{1}{\pi}\int_{-1}^{1}\left\{1-\beta^2\left[\frac{1-s^2}{1-x^2}\right]^{1/2}\right\}\frac{f(x^*)\,dx^*}{x^*-x^*} - \frac{A}{\pi}\left\{[(1-s^2)^{1/2}\right.$$

$$-(1-a^2)^{1/2}](1-\beta^2)\ln\left|\frac{a+s}{a-s}\right| + [\beta^2(1-a^2)^{1/2}$$

$$+(1-s^2)^{1/2}]\ln\frac{1-as+[(1-a^2)(1-s^2)]^{1/2}}{1+as+[(1-a^2)(1-s^2)]^{1/2}} - \beta^2(1-s^2)^{1/2}$$

$$\left.\times\ln\frac{1-s}{1+s} - 2s\cos^{-1}a\right\} - \frac{T\beta}{\pi(1-a)}\left[(s-a)\ln\frac{1-as+[(1-a^2)(1-s^2)]^{1/2}}{|a-s|}\right.$$

$$\left.+(s+a)\ln\frac{1+as+[(1-a^2)(1-s^2)]^{1/2}}{|a+s|}\right] \tag{3.22}$$

4. Pressure loading–CSS formulation and solution

The CSS formulation differs from the CNS formulation only in the manner in which the boundary conditions are prescribed in the zone of cohesive stresses. In the CSS formulation the tangential shear stress and the normal interface separation are prescribed in this region.

The boundary conditions for the CSS formulation are given by equation (2.1a,b), (2.4a,b) and (2.5a,b), while equations (2.2) and (2.3) are replaced by

$$a<|x|<L,\ y=0: \qquad \sigma_{xy}^1 = \sigma_{xy}^2 = \operatorname{sgn}(x)S\frac{|x|-a}{L-a} \tag{4.1}$$

$$\frac{\partial}{\partial x}(u_y^1 - u_y^2) = -B(1-x^2/L^2)^{1/2}\operatorname{sgn}(x) \tag{4.2}$$

Here, S is the maximum value of the shear cohesive stress (linear for $a<|x|<L$) and B is a constant to be determined.

We now follow the same procedure as was used in the solution for the CNS formulation. For convenience, the same notation is used for the definition of integral transforms given by equations (2.15), (2.16), and (2.27), (2.28), and for the dislocation densities, equations (2.32), (2.33). If the same steps are performed, with the difference in boundary conditions noted for the cohesive zone, equations (4.1) and

(4.2), then the following singular integral equations result.

$$\beta b_2(x)-\frac{1}{\pi}\int_{-1}^{1}\frac{b_1(t)\,dt}{t-x}=1, \qquad |x|<a \tag{4.3}$$

$$b_1(x)=-\operatorname{sgn}(x)B(1-x^2)^{1/2}, \qquad a<|x|<1 \tag{4.4}$$

$$\beta b_1(x)+\frac{1}{\pi}\int_{-1}^{1}\frac{b_2(t)\,dt}{t-x}=\begin{cases}0, & |x|<a\\ \operatorname{sgn}(x)\,S\dfrac{|x|-a}{1-a}, & a<|x|<1\end{cases} \tag{4.5}$$

Equations (4.3) and (4.4) can be combined to yield

$$\frac{1}{\pi}\int_{-a}^{a}\frac{b_1(t)\,dt}{t-x}=\beta b_2(x)-1+\frac{B}{\pi}\int_{a}^{1}(1-t^2)^{1/2}\,dt\left[\frac{1}{t+x}+\frac{1}{t-x}\right], \qquad 0<|x|<a \tag{4.6}$$

The conditions that $b_1(\pm a)$ is bounded and that the slip is single valued lead to the following equations:

$$\frac{\beta}{\pi}\int_{-a}^{a}\frac{b_2(x)\,dx}{(a^2-x^2)^{1/2}}+\frac{2B}{\pi}\{K[(1-a^2)^{1/2}]-E[(1-a^2)^{1/2}]\}-1=0 \tag{4.7}$$

$$\frac{1}{\pi}\int_{-1}^{1}b_2(x)\,dx=0 \tag{4.8}$$

Where $K(\cdot)$ and $E(\cdot)$ are complete elliptic integrals of the first and second kinds, respectively. The bounded solution to equation (4.6) is

$$b_1(s)=-\frac{\beta}{\pi}(a^2-s^2)^{1/2}\int_{-a}^{a}\frac{b_2(x)\,dx}{(a^2-x^2)^{1/2}(x-s)} -\frac{B}{\pi}(a^2-s^2)^{1/2}\int_{a}^{1}\left[\frac{1-t^2}{t^2-a^2}\right]^{1/2}\times\left[\frac{1}{t-s}-\frac{1}{t+s}\right]dt \qquad |s|<a \tag{4.9}$$

When equation (4.9) is put into equation (4.5) the problem is reduced to the singular integral equation given next:

$$\frac{1}{\pi}\int_{-1}^{1}\frac{b_2(t)\,dt}{t-s}=\frac{\beta^2(a^2-s^2)^{1/2}}{\pi}\int_{-a}^{a}\frac{b_2(t)\,dt}{(a^2-t^2)^{1/2}(t-s)} +\frac{\beta}{\pi}B(a^2-s^2)^{1/2}\times\int_{a}^{1}\left(\frac{1-t^2}{t^2-a^2}\right)^{1/2}\left[\frac{1}{t-s}-\frac{1}{t+s}\right]dt \qquad |s|<a$$

$$=\operatorname{sgn}(s)\left[\beta B(1-s^2)^{1/2}+S\frac{|s|-a}{1-a}\right], \qquad a<|s|<1 \tag{4.10}$$

Equation (4.10) is subject to conditions (4.7) and (4.8).

The numerical solution to these equations can be obtained in a manner similar to that described in Section 3. The unknowns to be solved for are $b_2(t)$, B, and S for a prescribed value of a. Equation (4.10) is put into discrete form by use of the Gauss–Chebyshev integration scheme as exploited by Erdogan and Gupta [9]. Thus,

let

$$b_i = b_2(t_i) \tag{4.11}$$

where

$$t_i = \cos\frac{\pi i}{2N+1}, \qquad i = 1, \ldots, N \tag{4.12}$$

and

$$s_k = \cos\frac{\pi(k-0.5)}{2N+1}, \qquad k = 1, \ldots N \tag{4.13}$$

Equation (4.10) can thus be written as

$$\frac{2s_k}{2N+1}\sum_{i=1}^{N} b_i \frac{(1-t_i^2)^{1/2}}{t_i^2 - s_k^2} = \begin{cases} \sum_{i=1}^{N} b_i G_i(s_k) + BI(s_k), & s_k < a \\ B\beta(1-s_k^2)^{1/2} + S\dfrac{s_k - a}{1-a}, & a < s_k < 1 \end{cases} \quad k = 1, \ldots, N \tag{4.14}$$

Here

$$G_i(s) = \frac{\beta^2[a^2 - s^2]^{1/2}}{N} \sum_{j=1}^{N} \frac{f_i(x_j) - f_i(s)}{x_j^2 - s^2} \tag{4.15}$$

$$x_j = a\cos[\pi(j - \tfrac{1}{2})/2N], \qquad j = 1, \ldots, N \tag{4.16}$$

where $f_i(x)$ are the functions used for interpolation, i.e.

$$b_2(x) = \sum_{i=1}^{N} b_i f_i(x), \tag{4.17}$$

and

$$f_i(x) = \frac{1}{2N+1}\left[\frac{\sin 2N(\theta_i - \theta)}{\sin(\theta_i - \theta)} - \frac{\sin 2N(\theta_i + \theta)}{\sin(\theta_i + \theta)}\right], \tag{4.18}$$

$$\theta_i = \frac{i\pi}{2N+1}, \qquad \theta = \cos^{-1}x \tag{4.19}$$

and

$$I(s) = \frac{\beta(a^2 - s^2)^{1/2}}{\pi} \int_a^1 \left[\frac{1-t^2}{t^2 - a^2}\right]^{1/2} \left[\frac{1}{t-s} - \frac{1}{t+s}\right] dt, \tag{4.20}$$

We note that equation (4.20) is not easily evaluated in the form shown and additional preparation is required for efficient numerical analysis (see Appendix I). Conditions (4.7) and (4.8) become

$$\sum_{i=1}^{N} b_i \left[\frac{\beta}{N}\sum_{j=1}^{N} f_i(x_i)\right] + B\frac{2}{\pi}\{K[(1-a^2)^{1/2}] - E[(1-a^2)^{1/2}]\} = 1 \tag{4.21}$$

$$\sum_{i=1}^{N} b_i(1-t_i^2)^{1/2} = 0 \tag{4.22}$$

From the indicated numerical technique given by equations (4.14)–(4.22) it is possible to obtain the desired quantities $b_2(t_i)$, for values of t_i given by equations (4.12), B, and S for given values of a and β. From these values the dislocation density, $b_1(t)$, can be found from the equation

$$b_1(s)=\begin{cases} -\dfrac{\beta(a^2-s^2)^{1/2}}{\pi}\displaystyle\int_{-a}^{a}\frac{b_2(x)-b_2(s)}{x-s}\frac{dx}{(a^2-x^2)^{1/2}}- \\ \dfrac{B(a^2-s^2)^{1/2}}{\pi}\displaystyle\int_{a}^{1}\left(\frac{1-t^2}{t^2-a^2}\right)^{1/2}\left[\frac{1}{t-s}-\frac{1}{t+s}\right]dt, \qquad |s|<a \\ -B(1-s^2)^{1/2}\operatorname{sgn}(s) \qquad a<|s|<1 \end{cases} \tag{4.23}$$

The stresses are given as

$$\frac{\sigma_y}{\sigma_0}=\begin{cases} -1, \qquad |s|<a \\ -1-\operatorname{sgn}(s)(s^2-a^2)^{1/2}\left[\dfrac{\beta}{\pi}\displaystyle\int_{-a}^{a}\frac{b_2(x)-b_2(s)}{x-s}\frac{dx}{(a^2-x^2)^{1/2}}\right. \\ \qquad\qquad \left.+\dfrac{B}{\pi}\displaystyle\int_{a}^{1}\left(\frac{1-t^2}{t^2-a^2}\right)^{1/2}\left(\frac{1}{t-s}-\frac{1}{t+s}\right)dt\right], \qquad |s|>a \end{cases} \tag{4.24}$$

$$\frac{\sigma_{xy}}{\sigma_0}=\begin{cases} 0, \qquad |s|<a \\ S\dfrac{|s|-a}{1-a}\operatorname{sgn}(s), \qquad a<|s|<1 \end{cases} \tag{4.25}$$

5. Numerical results for pressure loading

It is instructive at this point to obtain numerical results for the problem of uniform pressure loading. Since the calculation of bond failure under given applied loading is of major physical importance, the determination of a suitable failure criterion is the primary goal. The preceding sections have introduced cohesive stress zones at the tip of the crack by the CNS and CSS formulations, for which the boundary conditions differed only in the region of the bond in which cohesive stresses were assumed, $a<|x|<L$. If the two models are consistent, then whatever failure criterion is used, the same prediction of failure of the bond should hold for both foundations. This requirement is verified through calculation of numerical results.

First, some of the physical quantities will be calculated. Figure 2 shows the normal crack opening displacement for $\tilde{\beta}=0.1$ for the CNS formulation. The loading is such that the length of the cohesive zone is about 5% of the length of the crack. From this figure it can be seen that there is no abrupt change of curvature in the crack opening displacement so that no singularities in the stresses will be present at the transition points. For these same values of $\tilde{\beta}$ and σ_0 the shear stress distribution in the cohesive zone is plotted in Figure 3. Although the crack opening displacement and shear stress distribution might vary in magnitude due to the different values of $\tilde{\beta}$ and

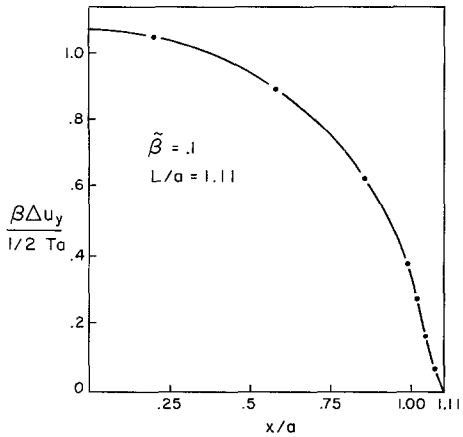

Figure 2. Crack opening displacements including separation in cohesive zone ($\tilde{\beta} = .1$).

σ_0, their form usually remained the same. Results of a similar nature are to be found for the CSS formulation. However, the CSS formulation exhibits normal and shear stress distributions in the cohesive zones that are roughly the reverse of those for the CNS formulation.

Figure 4 shows a plot of the *extent* of the cohesive zone compared with the crack length, $(L-a)/a$, given as a function of the applied loading, $\sigma_0/\hat{\sigma}_y$, where σ_0 has been normalized with respect to the average value of the *normal* cohesive stress, $\hat{\sigma}_y$.

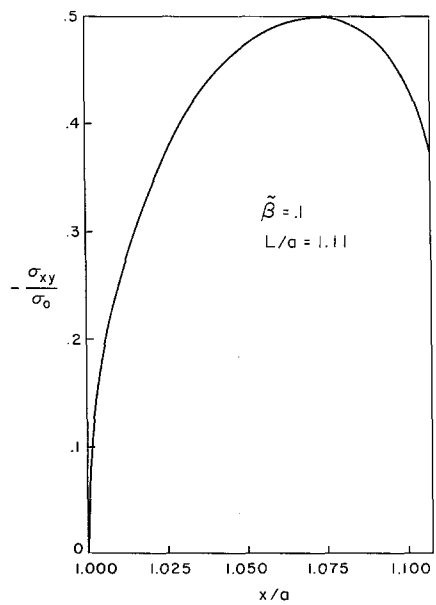

Figure 3. Shear stress distribution in the cohesive zone ($\tilde{\beta} = 0.1$).

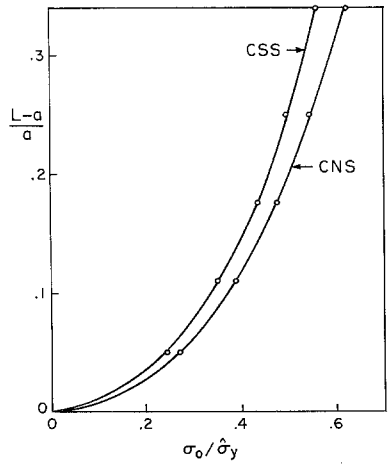

Figure 4. Comparison of the sizes of cohesive zones between CNS and CSS formulation.

We note that $\hat{\sigma}_y$ is given by the following expression:

$$\hat{\sigma}_y = \frac{1}{L-a}\int_a^L (\sigma_y + \sigma_0)\, dx \quad (=\tfrac{1}{2}T \quad \text{for CNS formulation}) \tag{5.1}$$

and that the average cohesive stress is calculated for the case where the crack is opened by a uniform tension of σ_0 at $y = \pm\infty$. As the loading is increased the difference in size between the two cohesive zones for the CNS and CSS formulations becomes larger. It appears from the figure that if the same ratio of L/a is taken for the CNS and CSS problems $\hat{\sigma}_y$ will be larger for the CSS problem than for the CNS problem. Therefore, the size of the cohesive zone would not appear to be a good quantity to use as a failure criterion.

Several other criteria were considered for the prediction of failure of the bond, but

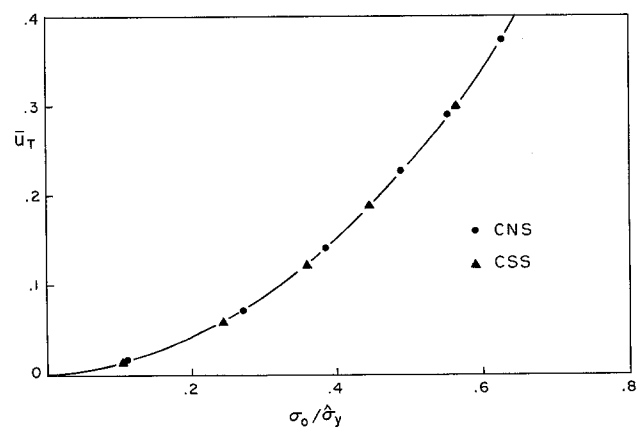

Figure 5. Crack tip opening displacement $u_T(\tilde{\beta} = 0.1)$.

only the one finally used will be mentioned here. It should be noted that the problem is basically nonlinear and that the traction and displacement in the cohesive zone will have components of Mode I and II present. The most reasonable form of failure criterion appeared to be the total interface separation at the trailing edge of the cohesive zone, i.e. at $x = \pm a$. This displacement jump is a quantity in which the normal and tangential components of the interface separation are added vectorially. It is physically realistic to postulate a fibre at the trailing edge of the cohesive zone that is stretched until a certain critical value is reached at which point it breaks. For both the CNS and the CSS formulation Figure 5 shows the relationship between $\tilde{u}_T$, (where $\tilde{u}_T = \beta u_T/\hat{\sigma}_y$), where u_T is the vector sum of the normal and tangential crack opening displacements at $x = \pm a$. From the figure it can be seen that the results for both formulations plot on the same curve. Thus, one has confidence that whichever formulation CNS or CSS, is used in the analysis, the results will be the same if the criterion for bond failure of a maximum interface separation at the trailing edge of the cohesive zone is postulated. In the sequel when the *combined* problem is solved, the solution technique for the CNS formulation only will be used.

For different values of $\tilde{\beta}$ curves of the type shown in Figure 5 can now be computed. Then, for specific values of a and $\tilde{\beta}$, and if the critical magnitude of u_T, $(u_T)_{cr}$, and the maximum value of the cohesive stress, T, are known, $(\tilde{u}_T)_{cr}$ will plot as a horizontal line. The intersection of the horizontal line with the corresponding curve of the type shown in Figure 5 yields the critical value of σ_0 for the given values of $(u_T)_{cr}$, T, a and $\tilde{\beta}$.

6. Shear loading

The case of uniform shear can be obtained from that of normal loading simply by a redefinition of dislocation densities as shown in the Table 1. Thus, to find physical quantities for shear loading one takes the entry in the normal loading column and replaces it by the entry (in the same row) in the shear loading column.

The symmetry of the problem will cause the faces of the crack to overlap over half of the crack length; in the practical case there will not be overlap, but instead, the crack faces will contact each other.

For the present analysis shear will be introduced, but only in the presence of a normal stress sufficiently large that overlap does not occur.

TABLE 1
Redefinition of dislocation densities for shear loading

Normal loading	Shear loading
$b_1(x)$	$b_2(x)$
$b_2(x)$	$-b_1(x)$
σ_{xy}/σ_0	$-\sigma_y/\sigma_0$
σ_y/σ_0	σ_{xy}/σ_0

7. Combined loading–CNS formulation

The failure criterion assumed in this paper is that bond failure occurs when the total crack-tip interface separation exceeds a critical value. This criterion is very convenient because it specifies failure on the basis of the critical magnitude of a single quantity. As shown in Figure 5 numerical values for the crack-tip interface separation are the same for the CNS and CSS formulations. It is now reasonable to assume that this is also true for combined loading, and hence in this section only the CNS-formulation will be used.

The boundary conditions for the problem of combined loading no longer possess the symmetry of the previous cases. For the present analysis the cohesive zones have different lengths and the stresses present therein also have different magnitudes. Furthermore, when the problems of normal and shear loadings are considered simultaneously, there will be a range of loading parameters for which overlap may occur at one of the crack tips. The problem of overlap can be treated mathematically as a contact problem, as in a paper by Comninou [3], and the complications introduced will not be too great. However, if contact is assumed in the overlap region, then one should introduce friction. An analysis which includes friction is beyond the scope of this paper. Thus we will only consider the case of combined loading in a range of loading parameters for which the crack faces do not overlap.

For analytical convenience the origin of the xy-system is shifted from the midpoint of the crack to the midpoint of the line element consisting of the crack and the cohesive zones, see Figure 1(b). Thus the original crack is defined by $-a_1 \leq x \leq a_2$, where $a_1 + a_2 = 2a$, and the leading edges of the cohesive zones are defined by $|x| = L$. The boundary conditions at $y = 0$ can now be stated as follows:

$$-a_1 \leq x \leq a_2: \qquad \sigma_y^1 = \sigma_y^2 = -\sigma \tag{7.1}$$

$$\sigma_{xy}^1 = \sigma_{xy}^2 = -\tau \tag{7.2}$$

$$-L \leq x \leq -a_1: \qquad \sigma_y^1 = \sigma_y^2 = T\frac{-x-a_1}{L-a_1} - \sigma \tag{7.3}$$

$$\frac{\partial}{\partial x}(u_x^1 - u_x^2) = -A_1(1-x^2/L^2)^{1/2} \tag{7.4}$$

$$a_2 \leq x \leq L: \qquad \sigma_y^1 = \sigma_y^2 = T\frac{x-a_2}{L-a_2} - \sigma \tag{7.5}$$

$$\frac{\partial}{\partial x}(u_x^1 - u_x^2) = -A_2(1-x^2/L^2)^{1/2} \tag{7.6}$$

$$|x| > L: \qquad u_y^1 = u_y^2; \qquad u_x^1 = u_x^2 \tag{7.7a,b}$$

$$|x| \geq 0: \qquad \sigma_{xy}^1 = \sigma_{xy}^2, \qquad \sigma_y^1 = \sigma_y^2 \tag{7.8a,b}$$

Here, σ and τ represent the applied normal and shear stresses, and in the cohesive zone the nonsymmetrical nature of the problem implies coefficients, A_1 and A_2, are different in the right- and left-hand zones, respectively. By using the exponential

transforms, equations (2.6)–(2.10), together with the boundary conditions equations (7.1)–(7.8), and by following a procedure almost identical to that of Section 2, we can write the problem as one requiring the solution of the following equations in terms of dislocation densities, $b_1(x)$ and $b_2(x)$

$$\beta b_2(x)-\frac{1}{\pi}\int_{-1}^{1}\frac{b_1(t)\,dt}{t-x}=\begin{cases}1-T\dfrac{-x-a_1}{1-a_1}, & -1<x<-a_1\\ 1 & -a_1<x<a_2\\ 1-T\dfrac{x-a_2}{1-a_2}, & a_2<x<1\end{cases} \tag{7.9}$$

$$\beta b_1(x)+\frac{1}{\pi}\int_{-1}^{1}\frac{b_2(t)\,dt}{t-x}=-\tau, \qquad -a_1<x<a_2 \tag{7.10}$$

$$b_2(x)=-A_1(1-x^2)^{1/2} \qquad -1<x<-a_1 \tag{7.11}$$

$$b_2(x)=-A_2(1-x^2)^{1/2} \qquad a_2<x<1 \tag{7.12}$$

where, instead of equations (2.25) and (2.26),

$$\xi M(\xi)=\frac{1}{(2\pi)^{1/2}}\int_{-L}^{L}b_2(t)e^{i\xi t}\,dt \tag{7.13}$$

$$\xi N(\xi)=\frac{i}{(2\pi)^{1/2}}\int_{-L}^{L}b_1(t)e^{i\xi t}\,dt \tag{7.14}$$

have been used to obtain equations (7.9) and (7.10). Two additional conditions that must be satisfied by the dislocation densities are as follows:

$$\frac{1}{\pi}\int_{-1}^{1}b_1(x)\,dx=0 \tag{7.15}$$

$$\frac{1}{\pi}\int_{-1}^{1}b_2(x)\,dx=0 \tag{7.16}$$

Furthermore $b_1(\pm1)$ and $b_2(a_2)$, $b_2(-a_1)$ must all be bounded.

By regarding $b_2(x)$ as a known function, we solve equation (7.9) for $b_1(s)$ to obtain

$$b_1(s)=-\frac{\beta(1-s^2)^{1/2}}{\pi}\int_{-1}^{1}\frac{b_2(x)\,dx}{(1-x^2)^{1/2}(x-s)}-TG_1(s) \tag{7.17}$$

where

$$\begin{aligned}G_1(s)=\frac{1}{\pi(1-a_1)}\Bigg[&(s+a_1)\ln\frac{1+a_1s+[(1-a_1^2)(1-s^2)]^{1/2}}{|a_1+s|}-(1-s^2)^{1/2}\\ &\times\cos^{-1}a_1\Bigg]+\frac{1}{\pi(1-a_2)}\Bigg[(s-a_2)\ln\frac{1-a_2s+[(1-a_2^2)(1-s^2)]^{1/2}}{|a_2-s|}\\ &+(1-s^2)^{1/2}\cos^{-1}a_2\Bigg]\end{aligned} \tag{7.18}$$

Substitution of equation (7.17) into equation (7.10) leads to

$$\frac{1}{\pi}\int_{-1}^{1}[1-\beta^2[(1-s^2)/(1-x^2)]^{1/2}]\frac{b_2(x)\,dx}{x-s}-T\beta G_1(s)=-\tau \tag{7.19}$$

It is convenient to write $b_2(x)$ in the following form:

$$b_2(x)=\begin{cases} f(x)-\dfrac{1}{a_1+a_2}\{[A_2(1-a_2^2)^{1/2}-A_1(1-a_1^2)^{1/2}]x+a_1A_2(1-a_2^2)^{1/2} \\ \qquad +a_2A_1(1-a_1^2)^{1/2}]\} \qquad -a_1<x<a_2 \\ -A_1(1-x^2)^{1/2} \qquad -1<x<-a_1 \\ -A_2(1-x^2)^{1/2} \qquad a_2<x<1 \end{cases} \tag{7.20}$$

Then, equation (7.19) becomes

$$\frac{1-\beta^2}{\pi}\int_{-a_1}^{a_2}\frac{f(x)\,dx}{x-s}+\frac{\beta^2}{\pi}\int_{-a_1}^{a_2}\frac{1-[(1-s^2)/(1-x^2)]^{1/2}}{x-s}f(x)\,dx=\gamma(s) \tag{7.21}$$

where

$$\gamma(s)=-\tau+T\beta G_1(s)+A_1\gamma_1(s)+A_2\gamma_2(s) \tag{7.22}$$

$$\begin{aligned}\pi\gamma_1(s)=&(1-\beta^2)\left[(1-s^2)^{1/2}-\frac{a_2-s}{a_1+a_2}(1-a_1^2)^{1/2}\right]\ln|a_1+s|+(1-\beta^2)\frac{a_2-s}{a_1+a_2}\\ &\times(1-a_1^2)^{1/2}\ln|a_2-s|+\beta^2(1-s^2)^{1/2}\ln|1+s|\\ &+\frac{\beta^2[(1-a_1^2)(1-s^2)]^{1/2}}{a_1+a_2}(\sin^{-1}a_2+\sin^{-1}a_1)-(1-s^2)^{1/2}\ln\{1+a_1s\\ &+[(1-a_1^2)(1-s^2)]^{1/2}\}-s\cos^{-1}a_1+\beta^2(1-a_1^2)^{1/2}\frac{a_2-s}{a_1+a_2}\\ &\times\ln\frac{1-a_2s+[(1-a_2^2)(1-s^2)]^{1/2}}{1+a_1s+[(1-a_1^2)(1-s^2)]^{1/2}}\end{aligned} \tag{7.23}$$

$$\begin{aligned}\pi\gamma_2(s)=&-(1-\beta^2)\frac{s+a_1}{a_1+a_2}(1-a_2^2)^{1/2}\ln|a_1+s|+(1-\beta^2)\left[\frac{s+a_1}{a_1+a_2}(1-a_2^2)^{1/2}\right.\\ &\left.-(1-s^2)^{1/2}\right]\ln|a_2-s|-\beta^2(1-s^2)^{1/2}\ln|1-s|\\ &-\frac{\beta^2[(1-a_2^2)(1-s^2)]^{1/2}}{a_1+a_2}(\sin^{-1}a_2+\sin^{-1}a_1)+(1-s^2)^{1/2}\ln\{1-a_2s\\ &+[(1-a_2^2)(1-s^2)]^{1/2}\}-s\cos^{-1}a_2+\beta^2\frac{s+a_1}{a_1+a_2}(1-a_2^2)^{1/2}\\ &\times\ln\frac{1-a_2s+[(1-a_2^2)(1-s^2)]^{1/2}}{1+a_1s+[(1-a_1^2)(1-s^2)]^{1/2}}\end{aligned} \tag{7.24}$$

Dislocation density $b_1(x)$ can be expressed in terms of $f(x)$ as

$$b_1(s)=-\frac{\beta}{\pi}(1-s^2)^{1/2}\int_{-a_1}^{a_2}\frac{f(x)\,dx}{(1-x^2)^{1/2}(x-s)}-\frac{\beta}{\pi}\gamma_3(s)-TG_1(s) \tag{7.25}$$

where

$$\gamma_3(s)=\Bigg\{-A_1\ln\frac{a_1+s}{1+s}-A_2\ln\frac{1-s}{a_2-s}$$
$$-\frac{A_2(1-a_2^2)^{1/2}-A_1(1-a_1^2)^{1/2}}{a_1+a_2}\Bigg[\sin^{-1}a_1+\sin^{-1}a_2$$
$$-\frac{s}{(1-s^2)^{1/2}}\ln\frac{1-a_2s+[(1-s^2)(1-a_2^2)]^{1/2}}{a_2-s}$$
$$+\frac{s}{(1-s^2)^{1/2}}\ln\frac{1+a_1s+[(1-s^2)(1-a_1^2)]^{1/2}}{a_1+s}\Bigg]$$
$$\frac{a_1A_2(1-a_2^2)^{1/2}+a_2A_1(1-a_1^2)^{1/2}}{a_1+a_2}\frac{1}{(1-s^2)^{1/2}}$$
$$\times\Bigg[-\ln\frac{1-a_2s+[1-s^2)(1-a_2^2)]^{1/2}}{a_2-s}+\ln\frac{1+a_1s+[(1-s^2)(1-a_1^2)]^{1/2}}{a_1+s}\Bigg]\Bigg\}(1-s^2)^{1/2} \tag{7.26}$$

The condition of boundedness for $b_1(+1)$ and $b_1(-1)$ yields for equation (7.9)

$$\frac{\beta}{\pi}\int_{-1}^{1}\frac{b_2(x)\,dx}{(1-x^2)^{1/2}}+\frac{T}{\pi}\Bigg[\frac{(1-a_1^2)^{1/2}-a_1\cos^{-1}a_1}{1-a_1}$$
$$+\frac{(1-a_2^2)^{1/2}-a_2\cos^{-1}a_2}{1-a_2}\Bigg]=1 \tag{7.27}$$

which can be further reduced to

$$\frac{\beta}{\pi}\int_{-a_1}^{a_2}\frac{f(x)\,dx}{(1-x^2)^{1/2}}+\frac{\beta}{\pi}(A_1Q_1+A_2Q_2)+\frac{T}{\pi}Q_3=1 \tag{7.28}$$

where

$$Q_1=\frac{1}{a_1+a_2}\{(a_1+a_2)(1-a_1)+[(1-a_1^2)(1-a_2^2)]^{1/2}-(1-a_1^2)$$
$$+a_2(1-a_1^2)^{1/2}(\sin^{-1}a_1+\sin^{-1}a_2)\} \tag{7.29}$$

$$Q_2=\frac{1}{a_1+a_2}[(a_1+a_2)(1-a_2)+[(1-a_2^2)(1-a_1^2)]^{1/2}-(1-a_2^2)$$
$$+a_1(1-a_2^2)^{1/2}(\sin^{-1}a_1+\sin^{-1}a_2)] \tag{7.30}$$

$$Q_3=\frac{1}{1-a_1}[(1-a_1^2)^{1/2}-a_1\cos^{-1}a_1]+\frac{1}{1-a_2}[(1-a_2^2)^{1/2}-a_2\cos^{-1}a_2] \tag{7.31}$$

Condition (7.16) leads to

$$\frac{1}{\pi}\int_{-a_1}^{a_2} f(x)\,dx + Q_4 A_1 + Q_5 A_2 = 0 \tag{7.32}$$

where

$$Q_4 = -\frac{1}{2\pi}[(\cos^{-1}a_1 + a_2(1-a_1^2)^{1/2}] \tag{7.33}$$

$$Q_5 = -\frac{1}{2\pi}[(\cos^{-1}a_2 + a_1(1-a_2^2)^{1/2}] \tag{7.34}$$

Through the use of equation (7.20) and

$$\frac{1}{\pi}\int_{-1}^{1}\frac{x\,dx}{\sqrt{1-x^2}}\frac{1}{\pi}\int_{-1}^{1}\frac{b_1(t)\,dt}{t-x} = -\frac{1}{\pi}\int_{-1}^{1} b_1(t)\,dt \tag{7.35}$$

condition (7.15) implies

$$\frac{\beta}{\pi}\int_{-a_1}^{a_2}\frac{xf(x)\,dx}{(1-x^2)^{1/2}} + \frac{\beta}{\pi}(A_1 Q_6 + A_2 Q_7) + \frac{T}{\pi}Q_8 = 0 \tag{7.36}$$

where

$$\begin{aligned} Q_6 = {} & -\frac{1}{2}(a_1^2-1) - \frac{1}{2(a_1+a_2)}\{-(1-a_1^2)^{1/2}(\sin^{-1}a_1 + \sin^{-1}a_2) \\ & + (1-a_1^2)^{1/2}[a_2(1-a_2^2)^{1/2} + a_1(1-a_1^2)^{1/2}] - 2a_2(1-a_1^2)^{1/2} \\ & \times[(1-a_2^2)^{1/2} - (1-a_1^2)^{1/2}]\} \end{aligned} \tag{7.37}$$

$$\begin{aligned} Q_7 = {} & -\frac{1}{2}(1-a_2^2) - \frac{1}{2(a_1+a_2)}\{(1-a_2^2)^{1/2}(\sin^{-1}a_1 + \sin^{-1}a_2) \\ & - (1-a_2^2)^{1/2}[a_2(1-a_2^2)^{1/2} + a_1(1-a_1^2)^{1/2}] \\ & - 2a_1(1-a_2^2)^{1/2}[(1-a_2^2)^{1/2} - (1-a_1^2)^{1/2}]\} \end{aligned} \tag{7.38}$$

$$\begin{aligned} Q_8 = {} & \frac{1}{2(1-a_1)}[a_1(1-a_1^2)^{1/2} - \cos^{-1}a_1] \\ & + \frac{1}{2(1-a_2)}[\cos^{-1}a_2 - a_2(1-a_2^2)^{1/2}] \end{aligned} \tag{7.39}$$

The condition of boundedness for $f(-a_1)$ and $f(a_2)$, together with equation (7.21) yields

$$\begin{aligned} & \frac{1}{\pi}\int_{-a_1}^{a_2}\frac{\gamma(s)\,ds}{[(a_2-s)(a_1+s)]^{1/2}} - \frac{\beta^2}{\pi}\int_{-a_1}^{a_2} f(x)\,dx \\ & \qquad \left\{\frac{1}{\pi}\int_{-a_1}^{a_2}\frac{1-[(1-s^2)/(1-x^2)]^{1/2}}{x-s}\frac{ds}{[(a_2-s)(a_1+s)]^{1/2}}\right\} = 0 \end{aligned} \tag{7.40}$$

Equation (7.21), together with subsidiary conditions, equations (7.28), (7.32), (7.36),

and (7.40), can then be solved for $f(x)$ and four of the six parameters (i.e., τ, T, a_1, a_2, A_1, A_2). For the present analysis as in Section 3 it is convenient to specify a_1, a_2, to solve for $f(x)$ and the remaining four parameters, τ, T, A_1, A_2. Once these quantities are determined, then $b_1(x)$ can be calculated from equation (7.25).

8. Numerical results for combined loading

For the presentation of the results, the applied stresses for combined loading have been normalized with respect to the average normal stress in the cohesive zone, i.e.,

$$\bar{\sigma} = \sigma/\tfrac{1}{2}T, \qquad \bar{\tau} = \tau/\tfrac{1}{2}T \tag{8.1a,b}$$

In the computational scheme it is convenient to specify a_1, a_2, and $\tilde{\beta}$, and to compute the corresponding values of τ, T, A_1, and A_2. This procedure produces the curves shown in Figures 6–8. Each point on a curve a_1/L is constant (a_2/L is constant) corresponds to unique values of $\bar{\sigma}$, $\bar{\tau}$ and $a_2/L(a_1/L)$. For prescribed $\bar{\sigma}$, $\bar{\tau}$ the corresponding a_1/L and a_2/L can now be found by interpolation from the curves shown in Figures 6–8. The curves in Figures 6–8 are cut off at values of $\bar{\tau}$ which separate the cases of contact and no contact. Thus, for small $\bar{\sigma}$, the shear stress $\bar{\tau}$ cannot be very high.

It can be easily shown from the directions of the applied loads that the crack-opening displacement at $x = a_2$ is larger than the one at $x = -a_1$. Once the parameters a_1/L, a_2/L, A_1 and A_2 have been determined, for given $\tilde{\beta}$, $\bar{\sigma}$ and $\bar{\tau}$, the total interface separation

$$u_T = [(\Delta u_x)^2 + (\Delta u_y)^2]^{1/2} \tag{8.2}$$

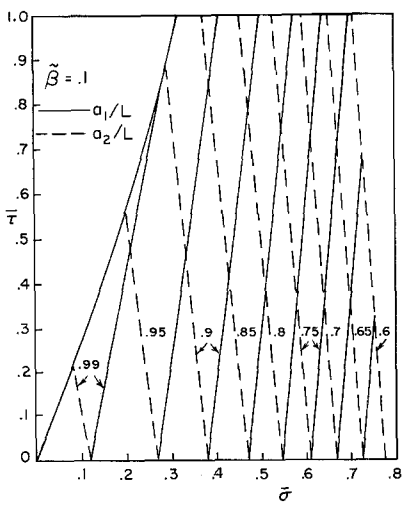

Figure 6. The extent of the cohesive zones for combined loading ($\tilde{\beta} = 0.1$).

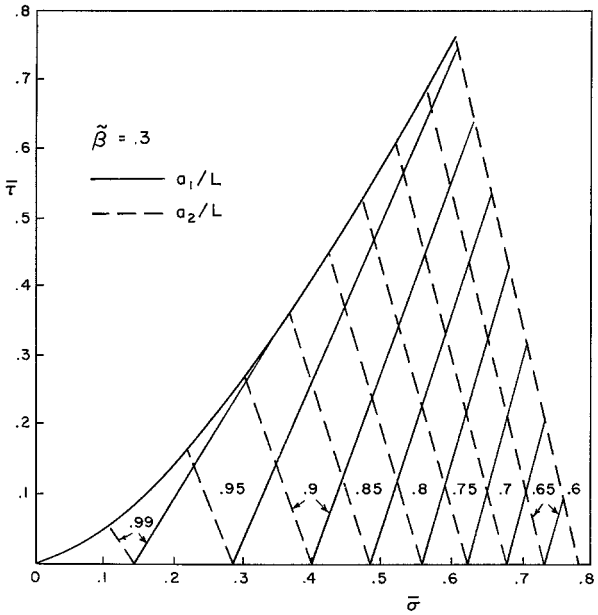

Figure 7. The extent of the cohesive zones for combined loading ($\tilde{\beta} = 0.3$).

at the critical crack tip $x = a_2$ can be calculated. It is then possible to plot curves in the $\bar{\sigma}\bar{\tau}$-plane corresponding to specified values of $\bar{u}_T$, where $\bar{u}_T = \beta u_T / \frac{1}{2}(a_1 + a_2)T$. Sets of such curves are shown in Figures 9–11.

For a given critical value of u_T (which defines the crack propagation criterion), Figures 9–11 show the domains of allowable applied stresses in the $\bar{\sigma}\bar{\tau}$-plane. These domains are bounded by $\bar{\tau} = 0$, $\bar{u}_T = (\bar{u}_T)_{\text{crit}}$ and the curve representing the maximum allowable $\bar{\tau}$ for which contact will not occur. As stated earlier, the case of contact of

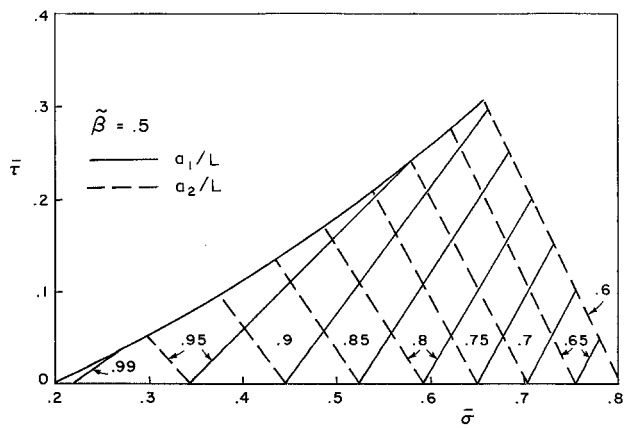

Figure 8. The extent of the cohesive zones for combined loading ($\tilde{\beta} = 0.5$).

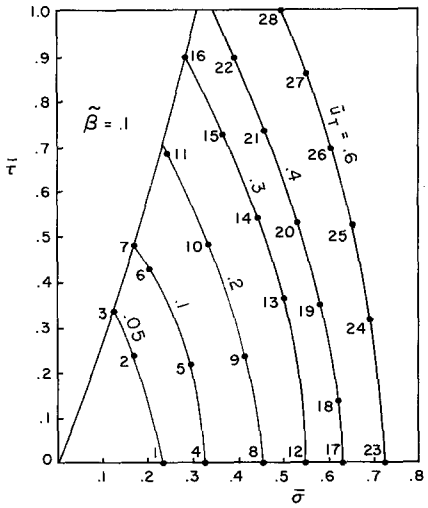

Figure 9. Contours for constant crack tip opening displacement u_T for combined loading ($\tilde{\beta} = 0.1$).

the crack faces requires special considerations which are beyond the scope of this paper. It can be seen that the magnitude of $\bar{\tau}/\bar{\sigma}$ for which contact does not occur depends on $\tilde{\beta}$, with smaller values of $\tilde{\beta}$ allowing a larger value of $\bar{\tau}/\bar{\sigma}$ without crack-face contact.

For a number of specific points which are indicated in Figure 9, the lengths of the cohesive zones have been tabulated in Table 2.

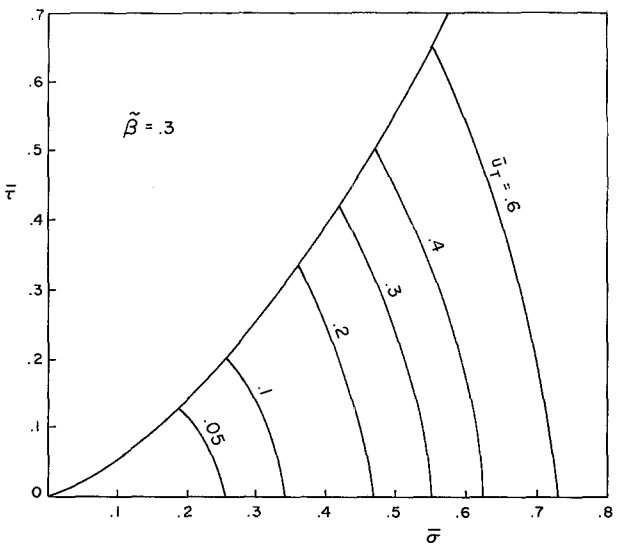

Figure 10. Contours for constant crack tip opening displacement u_T for combined loading ($\tilde{\beta} = 0.3$).

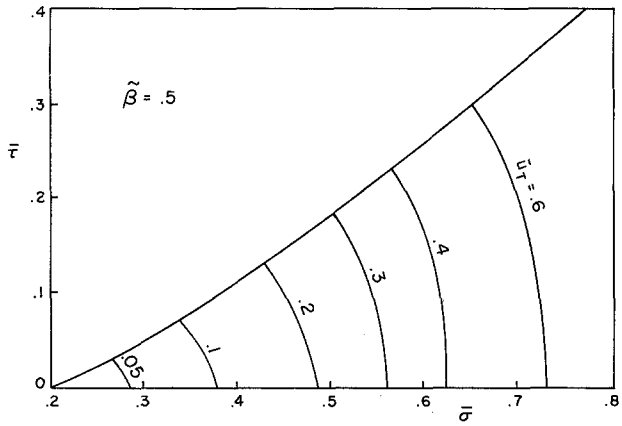

Figure 11. Contours for constant crack tip opening displacement u_T for combined loading ($\tilde{\beta} = 0.5$).

9. Conclusions

The goal of the present work is to construct a model for adhesive bond failure at the tip of an interface crack. The model is based on the assumption that there are bounded normal and tangential cohesive stresses in a zone near the tip of the crack. In the specification of such zones it is required that *all* stresses in the two materials are bounded.

The model chosen is seen to provide the following results which tend to make it attractive from the point of view of applications:

(a) The criterion for failure of the adhesive bond, i.e. that the bond fiber at the crack tip which is the crack opening displacement at that point is not to exceed a maximum, seems to be independent of the distribution of cohesive stresses, but

TABLE 2
Cohesive zones at points defined in Figure 9

Point	$\frac{L-a_1}{a_1+a_2}$	$\frac{L-a_2}{a_1+a_2}$	Point	$\frac{L-a_1}{a_1+a_2}$	$\frac{L-a_2}{a_1+a_2}$	Point	$\frac{L-a_1}{a_1+a_2}$	$\frac{L-a_2}{a_1+a_2}$
1	0.021	0.021	11	0.005	0.042	20	0.092	0.135
2	0.005	0.015	12	0.125	0.125	21	0.058	0.111
3	0.003	0.010	13	0.090	0.114	22	0.028	0.089
4	0.043	0.043	14	0.058	0.098	23	0.270	0.270
5	0.027	0.037	15	0.027	0.071	24	0.222	0.259
6	0.005	0.026	16	0.005	0.053	25	0.175	0.224
7	0.004	0.020	17	0.185	0.185	26	0.133	0.200
8	0.088	0.088	18	0.170	0.190	27	0.095	0.171
9	0.056	0.073	19	0.129	0.161	28	0.067	0.145
10	0.027	0.057						

rather depends only upon their average values. This is seen in Figure 5, where two models (CNS and CSS) are used to determine the crack tip opening displacement. The resulting curves are essentially the same.

(b) The relative size of the cohesive zones, when compared with the crack length, tends to be of a magnitude that is reasonable from a physical standpoint. As can be seen from Figures 6–8 and from Table 2, the size of the cohesive zones ranges from 1% of the crack length to about 30% of the crack length. For an adhesive bond in which the bond has considerably less strength than the two solids these values seem consistent. One should be cautious, however; the specification of the dislocation density as given by equation (2.3) may be too severe for large cohesive zones and thus the length of the cohesive zone may have to be restricted to a value smaller than 30%, say perhaps 10%.

(c) We note from Figures 10–12 that the curves are broken off when contact on the crack faces will begin to occur. As the shear stress is increased relative to the normal stress the left-hand cohesive zone becomes smaller when compared with the right-hand one. If the curves were continued into the region when overlap occurs, then the nature of the problem would be changed in that one of the regions would have to include contact between the two crack faces. Since this contact should include friction, it was felt that considerations of this effect are beyond the scope of this analysis.

To conclude we observe that it appears that interface crack problems can be solved with the introduction of cohesive zones at the crack tips. Such zones extend from about 1% to about 10% of the crack length, and they involve both normal and shear tractions. A reasonable quantity to consider for specification of bond failure is the maximum extension of the bond fiber at the crack tip. For uniform tension this quantity is consistent for two alternate formulations, and for combined loading the numerical results also seem to be very reasonable.

Acknowledgement

The work reported here was carried out in the course of research sponsored by the U.S. Army Research Office–Durham under Grant DAAG29-78-G-0031 with Northwestern University. The authors are pleased to acknowledge helpful discussions with Professor Maria Comninou.

Appendix

To evaluate the integral in equation (4.18),

$$I(s)=\frac{\beta}{\pi}(a^2-s^2)^{1/2}\int_{a}^{1}\left[\frac{1-t^2}{t^2-a^2}\right]^{1/2}\left(\frac{1}{t-s}-\frac{1}{t+s}\right)dt,$$

we let $u = t^2$, then

$$I(s) = \frac{\beta s}{\pi}(a^2 - s^2)^{1/2}\left[\frac{1}{|s|}\int_{a^2}^{1}\left[\frac{1-u}{u-a^2}\right]^{1/2}\frac{du}{u-s^2} - \int_{a^2}^{1}\left[\frac{1-u}{u-a^2}\right]^{1/2}\frac{du}{u-s^2}\frac{u-|s|}{u\,|s|}\right]$$

$$= \beta\ \mathrm{sgn}\,(s)(a^2-s^2)^{1/2}\left[\frac{1}{\pi}\int_{a^2}^{1}\left[\frac{1-u}{u-a^2}\right]^{1/2}\frac{du}{u-s^2} - \frac{1}{\pi}\int_{a^2}^{1}\left[\frac{1-u}{u-a^2}\right]^{1/2}\frac{du}{u+|s|\,u^{1/2}}\right.$$

$$= \beta\ \mathrm{sgn}\,(s)(a^2-s^2)^{1/2}\left[\left(\frac{1-s^2}{a^2-s^2}\right)^{1/2} - 1 - J(s)\right]$$

The integral, $(J(s))$ can be evaluated by substituting $u = \frac{1}{2}(1-a^2)p + \frac{1}{2}(1+a^2)$ Then

$$J(s) = \frac{1}{\pi}\int_{-1}^{1}\left[\frac{1-p}{1+p}\right]^{1/2} g(p)\,dp = \sum_{i=1}^{N}\frac{2(1-p_i)}{2N+1}\,g(p_i)$$

where

$$g(p) = \frac{1-a^2}{2}\frac{1}{u+|s|\,u^{1/2}}, \qquad p_i = \cos\frac{2\pi i}{2N+1}$$

Thus

$$I(s) = \beta\ \mathrm{sgn}\,(s)\{(1-s^2)^{1/2} - (a^2-s^2)^{1/2}[1+J(s)]\}$$

REFERENCES

[1] England, A. H., A crack between dissimilar media, *J. Appl. Mech.* 32 (1965) 400–402.
[2] Malyshev, B. M., and Salganik, R. L., The strength of adhesive joints using the theory of fracture, *Int. J. Fracture Mech.* 1 (1965) 114–128.
[3] Comninou, M., The interface crack, *J. Appl. Mech.* 44 (1977) 631–636.
[4] Comninou, M., The interface crack in a shear field, *J. Appl. Mech.* 45 (1978) 287–290.
[5] Barenblatt, G. I., The mathematical theory of equilibrium of cracks in brittle fracture, *Advances in Appl. Mech.* 7 (1962) 55–129.
[6] Dugdale, D. S., Yielding of steel sheets containing slits, *J. Mech. Phys. Sol.* 8 (1960) 100–104.
[7] Bilby, B. A., Cottrell, A. H., and Swinden, K. H., The spread of plastic yield from a notch, *Proc. Roy. Soc.* A272 (1963) 304–310.
[8] Muskhelishvili, N. I., *Singular Integral Equations*, P. Noordhoff, Groningen 1953.
[9] Erdogan, F., and Gupta, G. D., On the numerical solution of singular integral equations, *Quart. Appl. Math.* 30 (1972) 525–534.